Syntheses, Crystal Structures, and Properties of the Three Novel Perselenoborates RbBSe$_3$, CsBSe$_3$, and TlBSe$_3$ with Polymeric Chain Anions

Arno Lindemann, Jörn Küper, Winfried Hamann, Joachim Kuchinke, Christian Köster, and Bernt Krebs[1]

Anorganisch-Chemisches Institut, Westfälische Wilhelms-Universität, Wilhelm-Klemm-Strasse 8, D-48149 Münster, Germany

The perselenoborates RbBSe$_3$ and CsBSe$_3$ can be prepared from the metal selenides, amorphous boron, and selenium, in the case of TlBSe$_3$ directly from the elements. The solid-state reactions were carried out in evacuated carbon-coated silica tubes at high temperatures. Single-crystal X-ray data were used to determine the crystal structures. Both alkali metal perselenoborates RbBSe$_3$ and CsBSe$_3$ crystallize in the monoclinic space group $P2_1/c$ (RbBSe$_3$: $a = 7.279(2)$ Å, $b = 12.385(3)$ Å, $c = 6.169(2)$ Å, $\beta = 105.67(3)°$, $Z = 4$, $R1 = 0.0373$, and $wR2(F^2) = 0.1000$; CsBSe$_3$: $a = 7.570(2)$ Å, $b = 12.791(4)$ Å, $c = 6.171(2)$ Å, $\beta = 107.09(2)°$, $Z = 4$, $R1 = 0.0332$, and $wR2(F^2) = 0.0751$), while the thallium perselenoborate TlBSe$_3$ crystallizes in the acentric monoclinic space group Ia (alternative setting to Cc) with the lattice constants $a = 6.166(2)$ Å, $b = 12.109(2)$ Å, $c = 7.031(2)$ Å, $\beta = 113.88(3)°$, $Z = 4$, $R1 = 0.0423$, and $wR2(F^2) = 0.1157$. All three compounds contain polymeric anionic chains of composition ([BSe$_3$]$^-$)$_n$ formed by spirocyclically fused nonplanar five-membered B$_2$Se$_3$ rings in which the boron atoms are in a tetrahedral BSe$_4$ coordination. Vibrational spectra of the new compounds were measured and X-ray powder patterns are reported. © 2001 Academic Press

Key Words: selenoborates; perselenoborates; solid state structures; boron; selenium; crystal structures.

INTRODUCTION

In recent years considerable progress in preparation techniques made the synthesis and characterization of a larger number of thio- and selenoborates possible (1, 2). The crystal structures of the compounds known today consist of various unique types of chalcogenoborate anions coordinating different metal cations. The observed structure principles show boron in three different chalcogen coordinations.

Binary boron sulfides and selenides (1, 3–5) as well as various thioborates and selenoborates contain anions in which trigonal–planar-coordinated boron is found. Small isolated units with a high negative charge like BS$_3^{3-}$ (6–8), BSe$_3^{3-}$ (9), B$_2$S$_4^{2-}$ (10), B$_2$S$_5^{2-}$ (11), or B$_3$S$_6^{3-}$ (8, 12–14) are characteristic structural motifs in nonoxidic chalcogenoborates of alkali and alkaline earth metals or of monovalent thallium.

For boron in a tetrahedral surrounding by sulfur or selenium a higher degree of condensation of BQ$_4$ monomers (Q = S, Se) occurs, but isolated BQ$_4^{5-}$ anions are hitherto unknown. The smallest oligomer is a tetrameric B$_4$S$_{10}^{8-}$ unit (15, 16); various polymeric chain (17, 18), layer (19, 20), and network structures (21–23) arise from condensation of BQ$_4$ entities. Recently a new structural feature was observed in boron chalcogen chemistry: novel [B$_{12}$(BSe$_3$)$_6$]$^{8-}$ anions have been found in the ternary and quaternary compounds M_8[B$_{12}$(BSe$_3$)$_6$] and Hg$_2$$M_4$[B$_{12}$(BSe$_3$)$_6$] ($M$ = Rb, Cs) (24, 25). These anions are built up by B$_{12}$-*closo*-clusters, which are completely saturated with selenium by six BSe$_3$ entities.

Besides these selenoborato-*closo*-dodecaborates only a few (per)selenoborates of the heavy alkali metals or of monovalent thallium are mentioned in the literature. The selenoborates Tl$_3$BSe$_3$ (9), Rb$_2$B$_2$Se$_7$ (2, 26), and Cs$_3$B$_3$Se$_{10}$ (2, 27) were characterized by single-crystal X-ray determination. Dembovskii *et al.* studied the system Tl–B–Se by DTA analysis and determined a phase diagram for the pseudobinary cross section B$_2$Se$_3$–Tl$_2$Se (28). In the paper three compounds of the proposed formulas TlBSe$_2$, Tl$_4$B$_2$Se$_5$, and Tl$_8$B$_2$Se$_7$ are discussed based on unindexed powder patterns.

In this work we report the syntheses, crystal structures, and properties of the three new perselenoborates RbBSe$_3$, CsBSe$_3$, and TlBSe$_3$. They are the first known boron selenium compounds with polymeric anionic chain structures of composition [(BSe$_3$)$^-$]$_n$.

EXPERIMENTAL SECTION

Synthesis

The synthesis of well-defined and highly pure boron–selenium compounds is rather difficult because of the high reactivity of *in situ* formed boron selenide towards a variety of container materials at elevated temperatures. The fused silica tubes usually employed for solid-state reactions are attacked by boron selenide at temperatures above 650 K, forming silicon–selenium compounds by B–Si exchange at the surface of the ampoules, while annealing for a longer time leads to destruction of the attacked ampoules. For the synthesis of pure samples the reaction vessel must be made of either boron nitride or graphite, or silica tubes coated with glassy carbon must be used. The latter option is mostly applied. The reaction tubes can be prepared by slowly turning a silica ampoule filled with acetone vapour helically through the flame of an oxygen–hydrogen operated welding torch at about 1300 K. In some cases, especially when longer annealing is necessary, the former kind of crucible is employed. To protect them against oxidation they are welded into steel or tantalum ampoules under argon atmosphere, and these again are enclosed in evacuated silica tubes.

As starting materials the following products were used: elementary rubidium (Strem, 99 + %), elementary cesium (Strem, 99.5%), mercury selenide (Strem, 99.99%, PURAT-REM), elementary thallium granules (Alfa Aesar, 99.999%), amorphous boron (Alfa, amorphous powder, 95%), and selenium (Alfa, amorphous powder, 99.999%).

For the syntheses of RbBSe₃, CsBSe₃, and TlBSe₃ nearly stoichiometric amounts were mixed up and filled into carbon-coated silica tubes, which were thereafter sealed at a pressure of 6 Pa. The samples were heated in horizontal one-zone furnaces.

M₂Se (Rb, Cs). Samples were prepared by reaction of the elementary alkali metals and mercury selenide following instructions given by Klemm *et al.* (29).

RbBSe₃. A sample in the molar ratio of 1.2:2:4.5 of Rb₂Se, amorphous boron, and selenium was heated to 940 K within 8 h and kept at this temperature for 4 h. After cooling to 790 K for 4 h, the sample was annealed for an optimized crystallization process with a linear cooling rate to 520 K within 150 h. Orange–red plates and needles were obtained in quantitative yield.

CsBSe₃. A mixture in the molar ratio of 1:2:5 of Cs₂Se, amorphous boron, and selenium was heated to 970 K within 4 h and kept at this temperature for 2 h. After cooling, to 870 K for 10 h, and to 670 K for another 24 h, the sample was annealed for crystallization with linear cooling to 470 K within 120 h. Deep-red plate-shaped crystals were obtained in quantitative yield. The crystals cleave into fine

needles of parallel orientation on contact with a preparation needle.

TlBSe₃. A sample in the molar ratio of 1:1:2.9 of elementary thallium, amorphous boron, and selenium was heated to 950 K within 8 h and kept at this temperature for 4 h. After cooling during 16 h to 820 K, the sample was annealed for crystallization with linear cooling to 520 K within 120 h. Deep-red needles were obtained in quantitative yield. Again the crystals burst into very fine long needles of parallel orientation on contact with a preparation needle.

All products are air and moisture sensitive and were therefore handled under dry argon in a glove box.

Crystal Structure Analysis

For data collections single crystals of the three compounds were enclosed in sealed Mark capillaries under argon atmosphere. The X-ray diffraction data for RbBSe₃ and TlBSe₃ were collected using a STOE IPDS diffractometer. In the case of the CsBSe₃ the data collection was performed on a Siemens P3 four-circle diffractometer. The space groups were determined from systematic absences and intensity statistics. The resulting space groups were $P2_1/c$ for RbBSe₃ and CsBSe₃ and the space group Ia (transformed from the standard setting Cc because of the smaller monoclinic β angle) for the thallium perselenoborate. Structures were solved by direct statistical methods of phase determination using the SHELXTL PLUS program (30), and full-matrix least-squares refinements were done using the SHELXL-97 software program (31). In the refinement procedure for TlBSe₃ the resulting Flack parameter (32) gave a value of 0.22(2). The refinement of the crystal structure as a racemic twin was successful and yielded a conventional residual of $R1 = 0.0423$. The complete data collection parameters and details of the structure solutions and refinements are given in Table 1. The coordinates of all atoms, average temperature factors, and their estimated standard deviations are given in Table 2.

Further details of the crystal structure investigations may be obtained from the Fachinformationszentrum Karlsruhe, D-76344 Eggenstein-Leopoldshafen, Germany (fax: (+ 49)7247-808-666; e-mail: crysdata@fiz-karlsruhe.de) on quoting the depository numbers CSD-411343 (RbBSe₃), CSD-411342 (CsBSe₃), and CSD-411344 (TlBSe₃).

X-Ray Powder Diagrams, Vibrational Spectra, DSC

Powder diffraction patterns of RbBSe₃, CsBSe₃, and TlBSe₃ were measured with a STOE STADI P powder diffractometer using copper radiation ($\lambda = 1.540598$ Å) in 0.1-mm-diameter Mark capillaries. The observed XRD patterns were compared to calculated data resulting from

TABLE 1
Crystal Data, Details of Measurement, and Structure Solution for the Compounds RbBSe$_3$, CsBSe$_3$, and TlBSe$_3$

Empirical formula	RbBSe$_3$	CsBSe$_3$	TlBSe$_3$
Formula weight [g/mol]	333.16	380.60	452.06
Colour	orange–red	deep red	deep red
Crystal system	monoclinic	monoclinic	monoclinic
Space group	$P2_1/c$ (no. 14)	$P2_1/c$ (no. 14)	Ia (no. 9)
Lattice constants	$a = 7.279(2)$ Å	$a = 7.570(2)$ Å	$a = 6.166(2)$ Å
	$b = 12.385(3)$ Å	$b = 12.791(4)$ Å	$b = 12.109(2)$ Å
	$c = 6.169(2)$ Å	$c = 6.171(2)$ Å	$c = 7.031(2)$ Å
	$\beta = 105.67(3)°$	$\beta = 107.09(2)°$	$\beta = 113.88(3)°$
Cell volume	$535.5(2)$ Å^3	$571.1(3)$ Å^3	$480.1(2)$ Å^3
Formula units per cell	4	4	4
Calculated density	4.133 g/cm^3	4.426 g/cm^3	6.255 g/cm^3
Crystal dimensions	$0.32 \times 0.20 \times 0.16$ mm^3	$0.10 \times 0.09 \times 0.05$ mm^3	$0.12 \times 0.04 \times 0.04$ mm^3
Temperature	293(2) K	293(2) K	213(2) K
Diffractometer	STOE IPDS	SIEMENS P3	STOE IPDS
Radiation, wavelength	Mo$K\alpha$ ($\lambda = 0.71073$ Å)	Mo$K\alpha$ ($\lambda = 0.71073$ Å)	Mo$K\alpha$ ($\lambda = 0.71073$ Å)
Scan type	φ scan, 360°/0.8° step width	ω–2θ scan	φ scan, 360°/1.8° step width
$F(000)$	576	648	752
θ range for data collection	5.32° to 28.12°	2.82° to 26.99°	5.97° to 28.16°
Range in hkl	$-8 \leq h \leq 8$,	$-9 \leq h \leq 9$,	$-7 \leq h \leq 7$,
	$-16 \leq k \leq 16$,	$-16 \leq k \leq 0$,	$-16 \leq k \leq 16$,
	$-8 \leq l \leq 8$	$0 \leq l \leq 7$	$-9 \leq l \leq 9$
Total no. of reflections	9159	1363	4094
Independent reflections	1199 [R(int) = 0.0660]	1248 [R(int) = 0.0572]	1085 [R(int) = 0.0794]
Reflections with [$I > 2\sigma(I)$]	1075	933	1028
Absorption coefficient	29.5 mm^{-1}	25.4 mm^{-1}	56.2 mm^{-1}
Absorption correction	ABSCOR [37]	ψ scans	DECAY [37]
Data/restraints/parameters	1199/0/47	1248/0/47	1085/12/43
Refinement program	SHELXL-97 [31]	SHELXL-97 [31]	SHELXL-97 [31]
Refinement against	F_o^2	F_o^2	F_o^2
Residual indices	$R1 = 0.0373^a$	$R1 = 0.0332^a$	$R1 = 0.0423^a$
[$I > 2\sigma(I)$]	$wR2 = 0.0970^b$	$wR2 = 0.0698^b$	$wR2 = 0.1132^b$
Residual indices	$R1 = 0.0424$	$R1 = 0.0548$	$R1 = 0.0456$
(all data)	$wR2 = 0.1000$	$wR2 = 0.0751$	$wR2 = 0.1157$
Goodness of fit (GooF)^c	1.114	1.049	1.160
Extinction coefficient	0.0065(11)	0.0018(2)	0.0007(4)
Largest diff. peak and hole	1.14 and -1.34 eÅ^{-3}	1.66 and -1.34 eÅ^{-3}	2.10 and -3.01 eÅ^{-3}

$^a R1 = \sum \|F_o| - |F_c\|/\sum|F_o|$.
$^b wR2 = [\sum w(F_o^2 - F_c^2)^2/\sum w (F_o^2)^2]^{1/2}$.
$^c GooF = [(\sum w (F_o^2 - F_c^2)^2)/(n - m)]^{1/2}$.

single-crystal structure determinations using the STOE powder software package (38).

Infrared spectra were obtained on KBr pellets on a BRUKER IF 113 V FT-IR spectrometer in the range of 400 to 1000 cm^{-1}; accumulated FIR spectra (450 to 80 cm^{-1}) were recorded on polyethylene discs in a similar way in an evacuated sample chamber. Raman spectra were measured on a BRUKER IFS 66 spectrometer (with Raman Modul FRA 106) in sealed glass tubes.

DSC experiments were performed on a NETZSCH DSC 200 instrument, heating rate 10°/min.

The samples were prepared under argon in a glove box.

RESULTS AND DISCUSSION

Description of the Structures

The structures of the new perselenoborates RbBSe$_3$, CsBSe$_3$, and TlBSe$_3$ contain polymeric chain anions of general composition $[(BSe_3)^-]_n$ and coordinating metal cations M^+. The infinite one-dimensional anionic networks are formed from corner-sharing and nearly undistorted BSe$_4$ tetrahedra, which are additionally connected via one diselenide bridge. Every unit cell contains parts of two polymeric anions. In case of the two isotypic alkali metal perselenoborates a 2_1 screw axis along the crystallographic

TABLE 2

Atomic Coordinates and Isotropic Displacement Parameters (Å^2) for RbBSe₃, CsBSe₃, and TlBSe₃ with Standard Deviations

| Atom	x	y	z	$U_{eq}{}^a$
		RbBSe₃ in $P2_1/c$		
Rb(1)	0.25873(11)	0.42326(6)	0.20780(13)	0.0351(2)
Se(1)	0.94210(9)	0.17992(5)	0.17495(10)	0.0213(2)
Se(2)	0.80071(10)	0.41125(5)	0.33566(10)	0.0218(2)
Se(3)	0.53912(9)	0.19341(5)	0.35802(9)	0.0198(2)
B(1)	0.7017(10)	0.2687(6)	0.1760(10)	0.0185(12)
		CsBSe₃ in $P2_1/c$		
Cs(1)	0.26101(9)	0.42256(5)	0.21280(11)	0.0326(2)
Se(1)	0.93819(13)	0.18176(7)	0.16211(15)	0.0226(2)
Se(2)	0.79989(13)	0.40665(6)	0.31961(15)	0.0232(2)
Se(3)	0.54755(12)	0.19467(6)	0.33231(14)	0.0202(2)
B(1)	0.7056(14)	0.2693(7)	0.1534(16)	0.0184(19)
		TlBSe₃ in Ia		
Tl(1)	0.76104(11)	0.67554(5)	0.78902(10)	0.0320(3)
Se(1)	0.2472(3)	0.66737(12)	0.3608(3)	0.0208(4)
Se(2)	0.5305(2)	0.43361(16)	0.51192(18)	0.0178(4)
Se(3)	0.5127(3)	0.55269(12)	0.0693(2)	0.0179(3)
B(1)	0.329(3)	0.5239(11)	0.248(2)	0.013(3)

^{a} Defined as one third of the trace of the orthogonalized U_{ij} tensor.

b axis transforms the one-dimensional networks running parallel to [001] into each other. The diselenide units of the B₂Se₃ rings of these antiparallel chains are oriented in opposite directions (Fig. 1, right). In the crystal structure of the thallium perselenoborate the diselenide entities of all polymeric anions show the same orientation (Fig. 1, left),

this time oriented parallel to [100]. Accordingly a body-centered structure type with parallel anionic network units results.

There are remarkable structural similarities between the $[(BSe_3)^-]_n$ anion and polymeric boron diselenide $[BSe_2]_n$ (1, 4), which is built up by planar triselenadiborolane rings connected via exocyclic selenium atoms to form an infinite one-dimensional network. Assuming that boron diselenide is an intermediate product of the reaction to selenoborates the formation of polymeric anions in $MBSe_3$ (M = Rb, Cs, Tl) can be formally interpreted as a nucleophilic attack of diselenide anions to boron atoms of neighboring five-ring units in $[BSe_2]_n$ (Fig. 2). Due to the extension of the boron coordination ($sp^2 \rightarrow sp^3$) the $B_2Se_3Se_{2/2}$ rings in $[BSe_2]_n$ lose their planarity and two BSe_4 tetrahedra connected via one edge and one diselenide bridge are formed. The polymeric anions in $MBSe_3$ can also be described as a system of nonplanar five-membered B_2Se_3 rings spirocyclically fused via the boron atoms (Fig. 3).

The structural feature of the $[(BSe_3)^-]_n$ chains in the perselenoborates is a modified form of the chain structures called "Zweiereinfachketten" observed in silicate chemistry (33) and in compounds like $K_2SnS_3 \cdot 2 H_2O$ (34), $PbGeS_3$ (35), and Na_2GeS_3 (36). In thioborate chemistry the three isotypic compounds of formula MBS_3 (M = Rb, Cs, Tl) (2, 18, 27) exist, representing the same structure type as above. While the two alkali metal selenoborates RbBSe₃ and CsBSe₃ are isotypic to these analogous thioborates (space group $P2_1/c$) the thallium perselenoborate TlBSe₃ exhibits the same structural feature, but crystallizes in the acentric space group Ia. Further structural similarities can be found in the polymeric chain anions of the perchal-
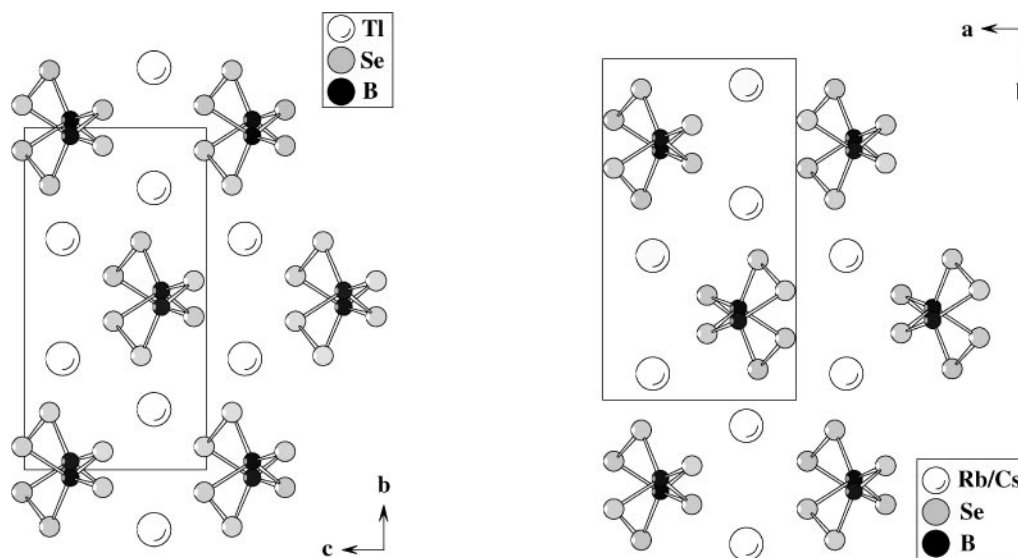
FIG. 1. Crystal structure of TlBSe₃ with parallel chains along [100] (left); crystal structure of $MBSe_3$ (M = Rb, Cs) containing polymeric antiparallel chains along [001] (right).
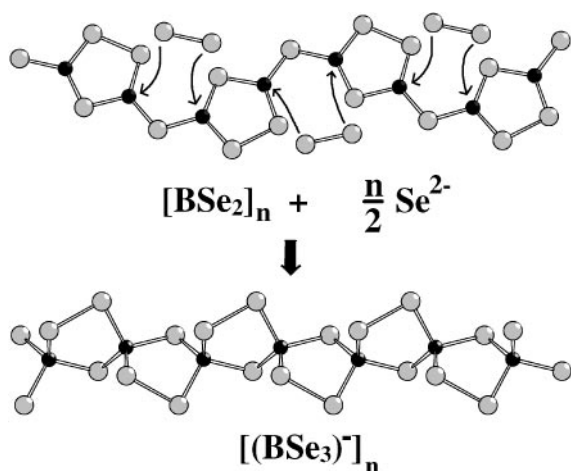
FIG. 2. Formal building mechanism of one-dimensional polymeric $[(BSe_3)^-]_n$-chain anions: nucleophilic attack of diselenide entities toward the binary boron selenide $[BSe_2]_n$.

coordinate the B_{12} cluster in the compounds $M_8[B_{12}(BSe_3)_6]$ and $Hg_2M_4[B_{12}(BSe_3)_6]$ ($M = $ Rb, Cs) (24, 25).

The Se–Se distances are fairly equal in all three perselenoborates. The average value of 2.355 Å is in very good agreement with those found in binary boron diselenide $[BSe_2]_n$ (2.347 Å) while the perselenoborates containing B_2Se_4 rings exhibit a slightly longer diselenide bridge (2.370 Å). The mean Se–B–Se angle in all the compounds amounts to 109.4(5)°, which agrees exactly with the ideal tetrahedral angle. Selected bond lengths and angles and the symmetry operations are given in Table 3.

Every cation connects three chain anions via ionic interactions. The coordination sphere of the alkali metal selenoborates consists of 12 selenium atoms forming an irregular MSe_{12} polyhedron. In case of TlBSe$_3$ the thallium cations are only 10-fold coordinated by selenium if Tl $\cdots$ Se distances up to 4 Å are considered. Figure 4 represents the

cogenoborates of composition $[(B_2Q_7)^{2-}]_n$ ($Q = S, Se$) (2, 17, 26) and $[(B_3Q_{10})^{3-}]_n$ (18, 27) in which five-membered B_2Se_3 and six-membered B_2Se_4 rings alternate in ratio 1:1 and 2:1, respectively.

The average B–Se bond lengths in the alkali metal perselenoborates $MBSe_3$ are calculated to be 2.060 Å (RbBSe$_3$) and 2.064 Å (CsBSe$_3$). In TlBSe$_3$ this bond distance is slightly shorter (2.058 Å) (the difference is hardly outside the limits of error), which can be explained by the low-temperature measurement. The mean bond lengths in all three compounds are significantly longer than those observed in perselenoborates of aforementioned compositions (Na$_2$B$_2$Se$_7$, 2.044 Å (17); K$_2$B$_2$Se$_7$, 2.050 Å (17); Rb$_2$B$_2$Se$_7$, 2.049 Å (2, 26); or Cs$_3$B$_3$Se$_{10}$, 2.05 Å (2, 27)). A comparison to bond lengths in selenoborates with trigonal–planar-coordinated boron indicates clear differences. The latter ones range from 1.90 Å (in $[BSe_2]_n$) to 2.02 Å in the BSe$_3$ ligands which
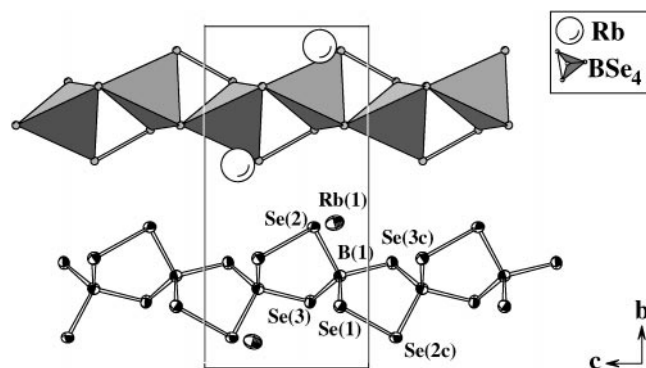
TABLE 3
Selected Bond Lengths (Å) and Angles (°) in the Structures of RbBSe$_3$, CsBSe$_3$, and TlBSe$_3$ with Standard Deviations

RbBSe$_3$			
B(1)–Se(1)	2.069(7)	Se(1)–B(1)–Se(3c)	112.8(3)
B(1)–Se(2)	2.055(7)	Se(2)–B(1)–Se(3)	107.8(3)
B(1)–Se(3)	2.061(7)	Se(2)–B(1)–Se(3c)	107.4(3)
B(1)–Se(3c)	2.053(6)	Se(3)–B(1)–Se(3c)	110.9(3)
Se(1)–Se(2c)	2.3562(10)	B(1)–Se(1)–Se(2c)	95.2(2)
Se(1)–B(1)–Se(2)	105.7(3)	B(1)–Se(2)–Se(1g)	91.5(2)
Se(1)–B(1)–Se(3)	111.8(3)	B(1)–Se(3)–B(1g)	98.6(3)
CsBSe$_3$			
B(1)–Se(1)	2.074(10)	Se(1)–B(1)–Se(3c)	113.4(4)
B(1)–Se(2)	2.053(9)	Se(2)–B(1)–Se(3)	107.3(4)
B(1)–Se(3)	2.083(9)	Se(2)–B(1)–Se(3c)	108.1(4)
B(1)–Se(3c)	2.044(10)	Se(3)–B(1)–Se(3c)	110.7(5)
Se(1)–Se(2c)	2.3541(14)	B(1)–Se(1)–Se(2c)	94.9(3)
Se(1)–B(1)–Se(2)	106.3(4)	B(1)–Se(2)–Se(1g)	92.0(3)
Se(1)–B(1)–Se(3)	110.7(4)	B(1)–Se(3)–B(1g)	98.4(4)
TlBSe$_3$			
B(1)–Se(1)	2.055(15)	Se(1)–B(1)–Se(3a)	107.2(7)
B(1)–Se(2)	2.076(14)	Se(2)–B(1)–Se(3)	111.4(7)
B(1)–Se(3)	2.034(17)	Se(2)–B(1)–Se(3a)	112.5(7)
B(1)–Se(3a)	2.065(14)	Se(3)–B(1)–Se(3a)	109.0(7)
Se(1)–Se(2a)	2.358(3)	B(1)–Se(1)–Se(2a)	90.5(4)
Se(1)–B(1)–Se(2)	104.6(6)	B(1)–Se(2)–Se(1b)	96.5(5)
Se(1)–B(1)–Se(3)	112.2(7)	B(1)–Se(3)–B(1b)	99.9(6)

Note. Symmetry operations for RbBSe$_3$ and CsBSe$_3$ in space group $P2_1/c$:

a	$1-x$	$1-y$	$-z$	e	$1-x$	$\frac{1}{2}+y$	$\frac{1}{2}-z$
b	$1-x$	$1-y$	$1-z$	f	$-1+x$	$\frac{1}{2}-y$	$-\frac{1}{2}+z$
c	x	$\frac{1}{2}-y$	$-\frac{1}{2}+z$	g	x	$\frac{1}{2}-y$	$\frac{1}{2}+z$
d	$-1+x$	y	z	h	$-1+x$	$\frac{1}{2}-y$	$\frac{1}{2}+z$

Symmetry operations for TlBSe$_3$ in space group Ia:

a	$-\frac{1}{2}+x$	$1-y$	z	e	$1+x$	y	$1+z$
b	$\frac{1}{2}+x$	$1-y$	z	f	$\frac{1}{2}+x$	$\frac{1}{2}+y$	$\frac{1}{2}+z$
c	x	$\frac{3}{2}-y$	$\frac{1}{2}+z$	g	x	y	$1+z$
d	$1+x$	$\frac{3}{2}-y$	$\frac{1}{2}+z$	h	$\frac{1}{2}+x$	$1-y$	$1+z$

FIG. 3. Unit cell of RbBSe$_3$ in ellipsoid and in tetrahedra representation (ellipsoids within 50% probability level).
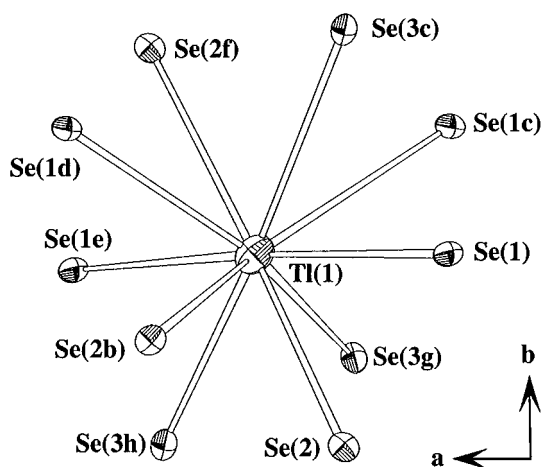
FIG. 4. View of the cation coordination of Tl(1) by selenium atoms in thallium perselenoborate TlBSe₃.

TABLE 4
Metal Selenium Coordination (Å) in the Structures of RbBSe₃, CsBSe₃, and TlBSe₃ with Standard Deviations

RbBSe₃			
Rb(1)···Se(1e)	3.6518(11)	Rb(1)···Se(2d)	3.6304(13)
Rb(1)···Se(1f)	3.6957(15)	Rb(1)···Se(2a)	3.8528(12)
Rb(1)···Se(1d)	3.7660(12)	Rb(1)···Se(3)	3.4793(12)
Rb(1)···Se(1h)	4.3402(14)	Rb(1)···Se(3c)	3.6452(12)
Rb(1)···Se(2)	3.8114(14)	Rb(1)···Se(3e)	3.7211(12)
Rb(1)···Se(2b)	3.6025(11)	Rb(1)···Se(3g)	4.2334(15)
CsBSe₃			
Cs(1)···Se(1d)	3.8868(14)	Cs(1)···Se(2b)	3.7540(14)
Cs(1)···Se(1f)	3.7974(15)	Cs(1)···Se(2a)	3.8587(14)
Cs(1)···Se(1e)	3.8139(14)	Cs(1)···Se(3)	3.5785(13)
Cs(1)···Se(1h)	4.4071(15)	Cs(1)···Se(3e)	3.8117(15)
Cs(1)···Se(2)	3.9416(16)	Cs(1)···Se(3c)	3.9320(13)
Cs(1)···Se(2d)	3.7434(15)	Cs(1)···Se(3g)	4.0859(16)
TlBSe₃			
Tl(1)···Se(1)	3.375(2)	Tl(1)···Se(2f)	3.588(2)
Tl(1)···Se(1d)	3.4111(18)	Tl(1)···Se(2b)	3.3051(18)
Tl(1)···Se(1c)	3.8996(19)	Tl(1)···Se(3g)	3.2992(18)
Tl(1)···Se(1e)	3.925(2)	Tl(1)···Se(3c)	3.6942(19)
Tl(1)···Se(2)	3.4866(19)	Tl(1)···Se(3h)	3.384(19)

Note. Symmetry codes are listed in Table 3.

cation coordination by selenium atoms in TlBSe₃. It is an interesting question whether the lone pair formally present in the thallium compound leads to any stereochemical activity visible in the coordination sphere as compared to the Rb and Cs species. However, on close inspection (Fig. 4) no hint to such an effect can be observed. A slight asymmetry might be detected in the rather long Tl···Se distances in the area of Se(1e), Se(1c), Se(3c), and Se(2f) as compared to shorter ones on the opposite side Se(2b), Se(3g), Se(1) (Fig. 4, Table 4). However, no correlation of this asymmetry can be seen to the loss of the inversion center on going from the structures of the rubidium and the cesium selenoborate to that of the thallium. The rubidium and cesium coordination by chalcogen in the alkali metal perselenoborates RbBSe₃ and CsBSe₃ is similar to that in the nonisotypic thallium compound. The metal selenium distances vary from 3.300 to 3.925 Å (mean: 3.537 Å) in thallium perselenoborate and range from 3.479 to 4.340 Å (mean: 3.786 Å) and from 3.578 to 4.407 Å (mean: 3.884 Å) in the rubidium and cesium compounds, respectively. The metal selenium distances are given in Table 4.

X-Ray Powder Diagrams, Vibrational Spectra

The agreement between observed and calculated powder diffraction data is very good despite the high absorption of all perselenoborates at copper radiation (TlBSe₃ exhibits a linear absorption coefficient of $\mu = 56.2$ mm⁻¹). As an example the recorded and simulated powder diagram of TlBSe₃ is shown in Fig. 5 in the 2θ range from 10° to 70°. In earlier physicochemical investigations performed by Dembovskii *et al.* on the quasibinary cross section B₂Se₃–Tl₂Se, powder patterns of three compounds with proposed compositions TlBSe₂, Tl₄B₂Se₅, and Tl₈B₂Se₇ were suggested

(28). A comparison with our powder pattern observed for TlBSe₃ reveals no similarities.

The strongest absorptions in the IR spectra are doublet bands at 574 and 554 cm⁻¹ for RbBSe₃ and at 567 and 548 cm⁻¹ for CsBSe₃ while the thallium perselenoborate shows one absorption peak at 574 cm⁻¹. These vibrations, of which some are also Raman active, i.e., bands are observed at 550 cm⁻¹ (RbBSe₃) and 578 cm⁻¹ (TlBSe₃), can be assigned to antisymmetrical B–Se stretching modes. Additional although less intense peaks occur at 641 cm⁻¹
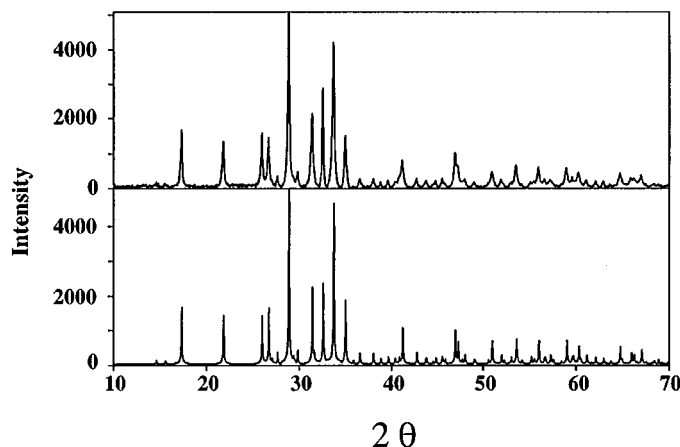

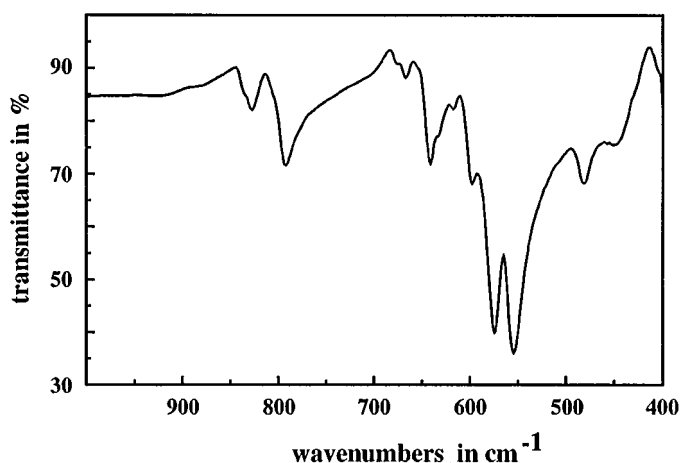**FIG. 5.** Observed (above) and calculated (below) powder patterns of TlBSe₃.

FIG. 6. IR spectrum of rubidium perselenoborate $RbBSe_3$.

(642) for the rubidium, $640 \, cm^{-1}$ for the cesium and $639 \, cm^{-1}$ (641) for the thallium compound in both IR and Raman spectra (the latter given in parentheses). A strong absorption band that is assignable to a symmetrical Se–Se stretching mode is observed in the region of $265 \, cm^{-1}$ ($RbBSe_3$) to $273 \, cm^{-1}$ ($TlBSe_3$) in the Raman spectra. Because of coupling effects of the light central atoms an assignment of further bands is not possible without normal coordinate analysis or theoretical calculations, which have not been available up to now. The infrared spectrum of the rubidium perselenoborate is represented in Fig. 6.

Unequivocally interpretable thermal analysis data could not be obtained for any of the compounds, but in the case of $TlBSe_3$ an endothermic effect is observed with an onset of 690 K and a maximum at 702 K. A corresponding exothermic peak (onset 685 K, minimum 683 K) occurs upon cooling. No similar behavior was found for either the rubidium or the cesium selenoborate.

ACKNOWLEDGMENTS

REFERENCES

1. B. Krebs, *Angew. Chem.* **95,** 113 (1983); *Angew. Chem. Int. Ed. Engl.* **22,** 113 (1983).
2. O. Conrad, C. Jansen, and B. Krebs, *Angew. Chem.* **110,** 3396 (1998); *Angew. Chem. Int. Ed.* **37,** 3208 (1998).
3. P. zum Hebel, H. Diercks, and B. Krebs, *Z. Kristallogr.* **185,** 40 (1988).
4. B. Krebs and H.-U. Hürter, *Acta Crystallogr. Sect. A* **37,** C163 (1981).
5. B. Krebs and H.-U. Hürter, *Angew. Chem.* **92,** 479 (1980); *Angew. Chem. Int. Ed. Engl.* **19,** 481 (1980).
6. P. Vinatier, P. Gravereau, M. Ménétrier, L. Trut, and A. Levasseur, *Acta Crystallogr. Sect. C* **50,** 1180 (1994).
7. F. Hiltmann, C. Jansen, and B. Krebs, *Z. Anorg. Allg. Chem.* **622,** 1508 (1996).
8. F. Hiltmann and B. Krebs, *Z. Anorg. Allg. Chem.* **621,** 424 (1995).
9. B. Krebs and W. Hamann, *J. Less-Common Met.* **137,** 143 (1988).
10. A. Hammerschmidt, C. Jansen, J. Küper, C. Püttmann, and B. Krebs, *Z. Anorg. Allg. Chem.* **621,** 1330 (1995).
11. C. Jansen, J. Küper, and B. Krebs, *Z. Anorg. Allg. Chem.* **621,** 1322 (1995).
12. C. Püttmann, H. Diercks, and B. Krebs, *Phosphorus Sulfur Silicon* **65,** 1 (1992).
13. F. Chopin and A. Hardy, *C. R. Acad. Sci.* **261,** 142 (1965).
14. F. Chopin and G. Turrell, *J. Mol. Struct.* **3,** 57 (1969).
15. P. Hagenmuller, F. Chopin, and B. Castagna, *C. R. Acad. Sci. C* **262,** 418 (1966).
16. A. Hardy, *Bull. Soc. Fr. Minéral. Cristallogr.* **91,** 111 (1968).
17. A. Hammerschmidt, J. Küper, L. Stork, and B. Krebs, *Z. Anorg. Allg. Chem.* **620,** 1898 (1994).
18. C. Püttmann, F. Hiltmann, W. Hamann, C. Brendel, and B. Krebs, *Z. Anorg. Allg. Chem.* **619,** 109 (1993).
19. F. Chopin and B. Capdepuy, *Bull. Soc. Chim. Fr.* 505 (1970).
20. C. Püttmann, W. Hamann, and B. Krebs, *Eur. J. Solid State Inorg. Chem.* **29,** 857 (1992).
21. P. zum Hebel, B. Krebs, M. Grüne, and W. Müller-Warmuth, *Solid State Ionics* **43,** 133 (1990).
22. B. Krebs and H. Diercks, *Z. Anorg. Allg. Chem.* **518,** 101 (1984).
23. A. Hammerschmidt, P. zum Hebel, F. Hiltmann, and B. Krebs, *Z. Anorg. Allg. Chem.* **622,** 76 (1996).
24. J. Küper, O. Conrad, and B. Krebs, *Angew. Chem.* **1997,** 109 (1995); *Angew. Chem. Int. Ed. Engl.* **36,** 1903 (1997).
25. A. Lindemann, J. Kuchinke, and B. Krebs, *Z. Anorg. Allg. Chem.* **625,** 1165 (1999).
26. C. Jansen, doctoral thesis, University of Münster (1997).
27. J. Küper, doctoral thesis, University of Münster (1996).
28. S. A. Dembovskii, V. V. Kirilenko, Yu. A. Buslaev, *Izv. Akad. Nauk SSSR Neorg. Mater.* **7,** 510 (1971); *Izv. Akad. Nauk USSR Neorg. Mater.* **8,** 237 (1972).
29. W. Klemm, H. Sodomann, and P. Langmesser, *Z. Anorg. Allg. Chem.* **241,** 281 (1939).
30. G. M. Sheldrick, SHELXTL PLUS, Siemens Analytical X-Ray Instruments, (1990).
31. G. M. Sheldrick, SHELXL-97, Program for the refinement of crystal structures, University of Göttingen (1997).
32. H. D. Flack, *Acta Crystallogr. Sect. A* **39,** 876 (1983).
33. F. Liebau, *Naturwissenschaften* **49,** 41 (1962).
34. W. Schiwy, C. Blutau, D. Gäthje, and B. Krebs, *Z. Anorg. Allg. Chem.* **412,** 1 (1975).
35. M. Ribes, J. Olivier-Fourcade, E. Philippot, and M. Maurin, *Acta Crystallogr. Sect. B* **30,** 1391 (1974).
36. J. Olivier-Fourcade, E. Philippot, M. Ribes, and M. Maurin, *Rev. Chim. Minér.* **9,** 757 (1972).
37. Stoe IPDS Software, Version 2.75, Stoe & Cie GmbH, (1996).
38. Stoe User Manual Version 5.2, (1990); Stoe & Cie GmbH, Powder Software User Manual Version 1.08, (1992).